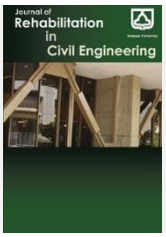

Journal of Rehabilitation in Civil Engineering

Journal homepage: https://civiljournal.semnan.ac.ir/

Numerical Study of Concentric Brace Equipped with the Eccentric Elements for Strengthening Buildings

Asadullah Attal [1,*]; Mohammad Ali Kafi [2]

1. Ph.D. Candidate, Faculty of Civil Engineering, University of Semnan, Semnan, Iran
2. Associate Professor, Faculty of Civil Engineering, University of Semnan, Semnan, Iran
Corresponding author: *mkafi@semnan.ac.ir*

ARTICLE INFO

Article history:
Received: 02 January 2023
Revised: 23 April 2023
Accepted: 05 July 2023

Keywords:
Ductility;
Concentric bracing;
Buckling;
Energy dissipation;
Seismic response;
Eccentrical innovative connection.

ABSTRACT

Concentric bracing with ease of design and execution and low construction cost represents the widely used system for resisting the structures to lateral forces. The diverse lateral load-bearing system has a variety of types, characterized by its main performance properties as bearing capacity, stiffness, performance ductility, and energy dissipation. Studies revealed that the brace system is a valuable option for retrofitting existing steel and reinforced concrete structures. However, the bracing system suffers a weakness called axial buckling of the brace under critical compressive load, reducing bearing capacity and interrupting energy dissipation. To address this imperfection and induce the seismic response of the concentrically braced frames, several methods proposed to optimize the performance of concentric braces as; using ductile connections, incorporating shear dissipators, hydraulic or mechanical dampers, frictional dissipators, and restrained braces to avoid buckling. Therefore, in this study, an innovative geometry of brace-to-frame connection is investigated to enhance the concentric brace's performance. The local dissipative fuse system is used to connect the steel channels with the gusset plate at one or both ends and at the time of the earthquake the dissipator yields before the brace buckles and forms a flexible plastic hinge, consuming a significant amount of earthquake energy. Similar studies have been performed earlier but the valuable tensional capacity of the braces was affected. Thus, the innovative method aims to maintain the tensional capacity of the brace in addition to buckling prevention and energy dissipation. Also, the dissipators have a post-earthquake ability to easily provide and replace. Consequently, the numerical work performed in this study effectively prevents buckling, and enhanced energy dissipation while maintaining the full tensional functionality of the brace.

E-ISSN: 2345-4423

How to cite this article:
Attal, A., & Kafi, M. A. (2024). Numerical Study of Concentric Brace Equipped with the Eccentric Elements for Strengthening Buildings. Journal of Rehabilitation in Civil Engineering, 12(1), 92-105. https://doi.org/10.22075/jrce.2023.29493.1786

1. Introduction and literature review

Seismic functional structures with concentric braces are a concern for the designer because of their deprived ductility [1]. Along with that, the proper performance behavior of concentric braces for lateral resisting system suggests appropriate stiffens, strength, and energy dissipation capability [2]. So, plentiful studies conducted to improve the performance behavior of the concentric braces and several methods have been proposed to improve the ductility and buckling vulnerability of concentric braces. Overall, active, passive, and semi-active control systems are considered to dissipate earthquake energy, while passive control methods represent the simplest and most economical mechanisms for resisting lateral forces [3–6]. Based on the recent earthquake guidelines and norms, a structure should experience inelastic behavior under moderate earthquake [7] Along with that, numeral passive energy dissipating systems are studied and reliable references are addressed to assess the outcome of the analysis and design of structures with passive energy dissipating system [8]. Also, local dissipative devices incorporated on braces successfully dissipated remarkable earthquake energy and reduced damage and loss of lives [3].

Hereafter, An experimental and numerical investigation was performed to evaluate concentric brace equipped with steel rings [9–11]. Another study incorporated steel a ring on diagonal brace and successfully improved its cyclic behavior. Steel rings are also used as performance improvers with off-center diagonal brace [12–14]. A diamond-shaped diagonal brace is linked with a steel ring for improving its cyclic performance behavior [15,16]. The circular yielding element and brace bars act inversely when a cyclic load is applied to the diagonal brace. In a different research, three types of connections; rigid, semi-rigid, and pinned were used to evaluate the system performance [15]. The result denoted that steel rings with slighter dimensions and thickness absorb more energy and represented enhanced resisting capacity.

In a different research, two types of dissipative brace to column connections; Pins (two types) and U shape devices evolved for absorbing earthquake energy [16,17]. Structural parameters such as the type of dissipative connections, the slimness of the bracing elements, the stiffness of the connection, or the thickness of the plates were keenly assessed. The study aims to develop design applied rules defining appropriate measurement for structural dissipative connections. Thus, steel frames incorporate with dissipator experimented for large plastic deformation without collapsing system functionality, performance, and dissipated energy [18,19].

A nonlinear finite element model was defined to evaluate the seismic behavior of the ring damper in the center diagonal brace using ABAQUS software [19]. Therefore, incorporating steel ring damper in brace systems caused enhanced early stiffness, bearing capacity, distortion, and energy absorption [11,14,18,20–22]. In a separate research steel ring filled with compressive plastic or high-performance fiber-reinforced concrete was incorporated into the connection of braces to enhance its performance behavior and dissipate earthquake energy [23,24]. The study performed under cyclic loading experimentally and numerically employing the finite element method ABAQUS software resulted in a wide range of hysteresis loops and amplified performance behavior. Likewise, a local eccentricity of brace-frame connection evaluated to address its effect on the nonlinear behavior of the concentric brace

[25–27].In addition, a study aimed to retrofit a reinforced concrete frame with concentric steel brace and eccentric steel brace to improve its performance [28,29].

Consequently, this study aims to improve the performance of concentric braces, through a device with an exclusive geometry that sustains non-elastic deformation and dissipate earthquake energy. The eccentrical yielding elements are incorporated in a connection joint of the brace to frame, dissipating earthquake energy and prevent buckling. The mechanism is considered as an innovative method to use most of the tensional capacity of concentric braces. Such eccentrical yielding elements concerning to the story drift can be installed in one or both end joints of the brace. The ductile zones as energy dissipators have been studied analytically based on finite element methods by ABACUS software resulted that a brace with eccentric elements subjected to cyclic loading presenting a steady and wide hysteretic curve and can easily prepare and replace. Analytical observations verified that the proposed local plastic mechanism caused the structural members to remain elastic. Furthermore, the destruction is restricted to the yielding elements with the capability to easily provide and replace when the waves are over.

2. Description of the eccentric yielding elements

Formed steel plates with the unique geometry connecting brace-frame joint through gusset plate to improve the performance. The two parts of circle conforms to a ring of semi-circle named C-shaped Dissipative Devices (CDD) Fig. 2. The thick c-shaped dissipators decentralize the earthquake force employed through the moment frame to the brace bar Fig. 1. The objective is to improve performance, dissipate energy, and prevent buckling while the full tensional capacity of the brace utilized.

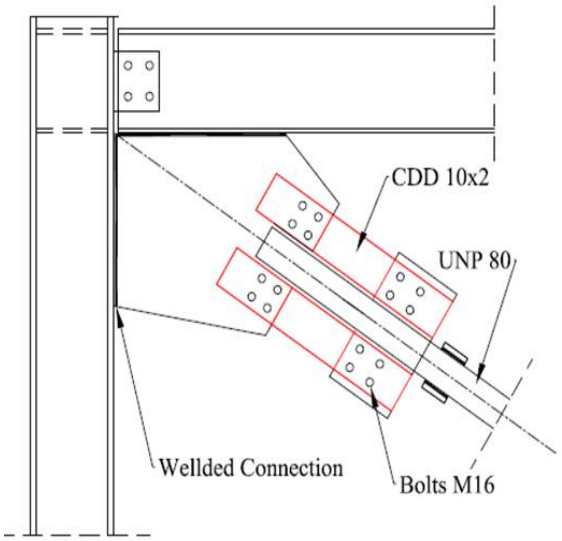

Fig. 1. Brace to frame connection.

The assigned geometry of CDD is designed to behave inelastically before the brace in compression and let the brace to yield in tension. That behavior improves earthquake energy dissipation and unlike other dissipators does not affect the tensional capacity of the brace.

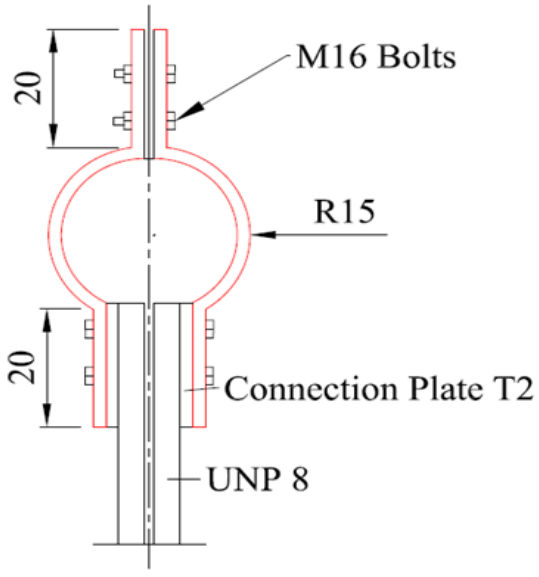

Fig. 2. Side view of CDD, units in cm.

The destruction during an earthquake is restricted to the CDD and shows large deformation and plastic hinges formed in

CDDs absorbing more energy compare to conventional concentric braces.

In addition, the dissipative devices provide a stable bed for welding and or bolted connection. Even though, the current draft in Fig. 1 and 2 is only mentioned as a bolted option.

A braced frame equipped with CDD type connection represents the following advantages compared to traditional braced steel frames:

- Compatibility with seismic design criteria
- Damage concentration only at CDDs
- Buckling prevention
- Contrary to other dissipators, CDD allows to use the full tensional the capacity of the brace
- The CDD remains functional in all cycles, even at huge story drifts
- Low-cost and easy replacement after the earthquake

3. The method of model analysis

In regard to examining the hysteretic behavior of concentric brace with embedded dissipative devices, a nonlinear static analysis with a displacement-controlled cyclic loading model is analyzed. The hysteretic loops of a Concentric Brace equipped with C shape Dissipative Devices (CB-CDD) are presented in Fig. 3 and finally compared with the performance of a Traditional Concentric Brace (TCB). The CB-CDD model is designed to optimize the system's ductility and avoid compressive buckling. Exclusively, this research aims to utilize the brace's full tensile functionality while preventing buckling under pressure. To accomplish this objective, the tensional capacity of dissipative devices should be more than the brace bars to let the brace use its full tensile functionality in tension and eccentrically deform before the brace buckle in compression.

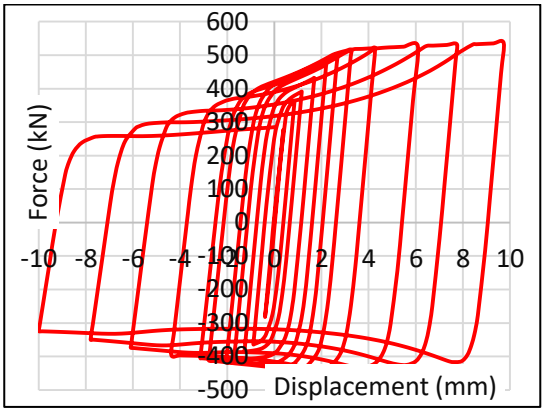

Fig. 3. Hysteresis Loops of CB with CDD.

The fact of using reduced bearing capacity is already considered in an experimental study by other researchers [2,9,12,14,25,26,28,30–33]. Fig.4 represents the test configuration of a steel ring used as fuse with reduced capacity.

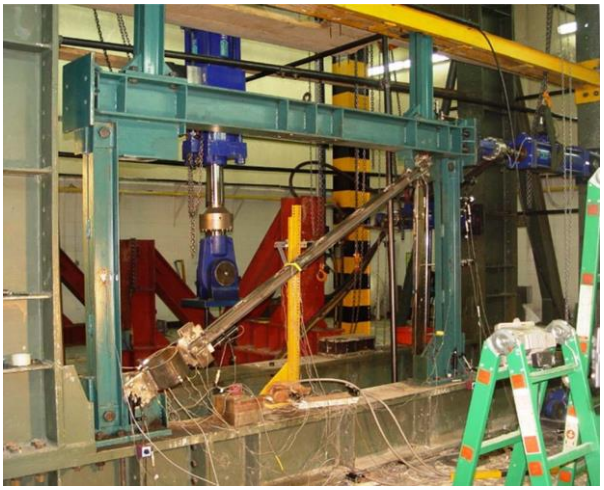

Fig. 4. Diagonal brace incorporated [12].

In this study, the rule of design is to increase the bearing capacity of dissipative devices and let the brace to yield in tension while the geometrical eccentricity cause to yield CDD before the brace buckle in compression. The buckle is controlled and limited only to the yielding elements and all other members remain elastically functional in compression. Eventually, the yielding elements are capable to be replaced for the next duty whenever lose its functionality.

4. Verification of numerical analysis with experimental data

A diagonal concentric brace with a steel ring as a yielding device incorporated in a one-floor single-bay steel frame experimented and the performance of the brace was improved successfully [29]. So, in this study the data of the experiment compared with the result of the numerical analysis to validate the software functionality Fig. 5. The dimensions of the yielding devices in the experiment in mm are T12, L150, and external R220 and initially cast from a steel plate. As presented the hysteretic loops attained from the numerical analysis well-matched the experimental data Fig. 5.

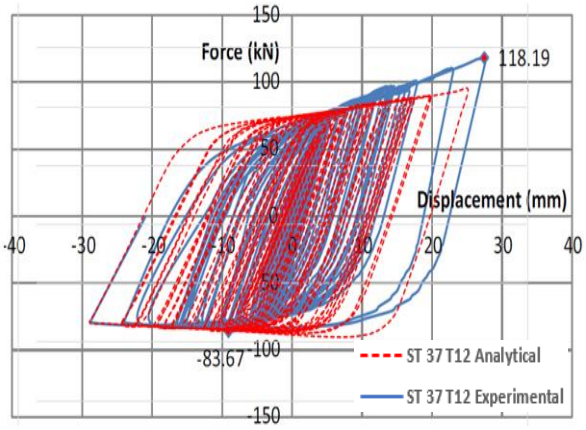

Fig. 5. Comparison of experimental and numerical hysteresis loops.

5. Load history

The cyclic load applied is symmetrical and is comparable to earthquake loads suggested by the method explained in code ATC-24 [34]. Based on the guideline provided by the code, the load history should follow the steps offered in Fig. 6. In this loading history, the steps noted as;

δ_i – Represents maximum load displacement

n_i – Loading cycles for specific δ_i

Δ - Displacement where the yielding elements start to yield

Thus, the loading history used for this specific model is presented in Table 1 and Fig. 7.

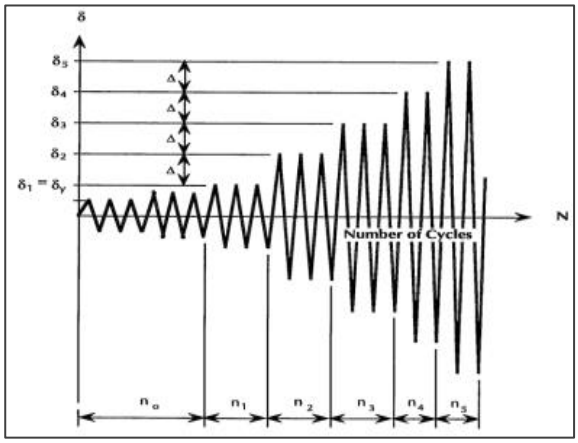

Fig. 6. Load history method in code ATC- 24.

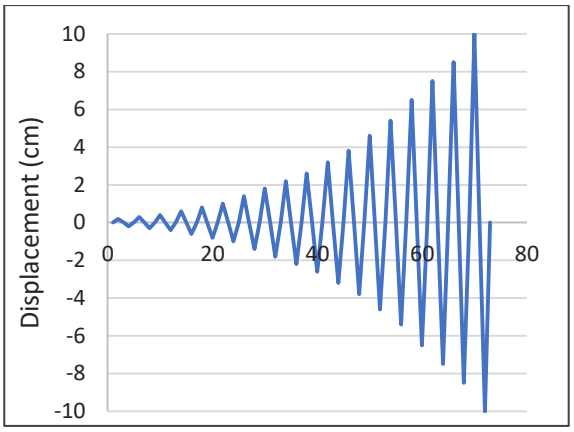

Fig. 7. Loading history for this model.

6. Performance of concentric brace equipped with CDD

The dissipative devices used in this model are named as T20L100R150, where the letters T, L, and R respectively represent dimensional properties as thickness, width, and curve ray all in mm. The outcome of applied cyclic load to the model plotted as force-displacement hysteretic loops presented in Fig. 8 and 9 denotes the hysteresis loops and performance envelope or backbone for the concentric brace supplied with CDD. The result indicates that the brace performance behavior effectively improved under cyclic loading, neglected to buckle, and used the full tensional capacity of the brace.

Table 1. Loading history used for the model.

Cycle	Displacement (mm)		Cycle	Displacement (mm)		Cycle	Displacement (mm)	
1	0	0	17	3.3	-3.3	33	6.82	-6.82
2	0.11	-0.11	18	3.52	-3.52	34	7.04	-7.04
3	0.22	-0.22	19	3.74	-3.74	35	7.26	-7.26
4	0.44	-0.44	20	3.96	-3.96	36	7.48	-7.48
5	0.66	-0.66	21	4.18	-4.18	37	7.7	-7.7
6	0.88	-0.88	22	4.4	-4.4	38	7.92	-7.92
7	1.1	-1.1	23	4.62	-4.62	39	8.14	-8.14
8	1.32	-1.32	24	4.84	-4.84	40	8.36	-8.38
9	1.54	-1.54	25	5.06	-5.06	41	8.58	-8.58
10	1.76	-1.76	26	5.28	-5.28	42	8.8	-8.8
11	1.98	-1.98	27	5.5	-5.5	43	9.02	-9.02
12	2.2	-2.2	28	5.72	-5.72	44	9.24	-9.24
13	2.42	-2.42	29	5.94	-4.94	45	9.46	-9.46
14	2.64	-2.64	30	6.16	-6.16	46	9.68	-9.68
15	2.86	-2.86	31	6.38	-6.38	47	9.9	-9.9
16	3.08	-3.08	32	6.6	-6.6	48	10	-10

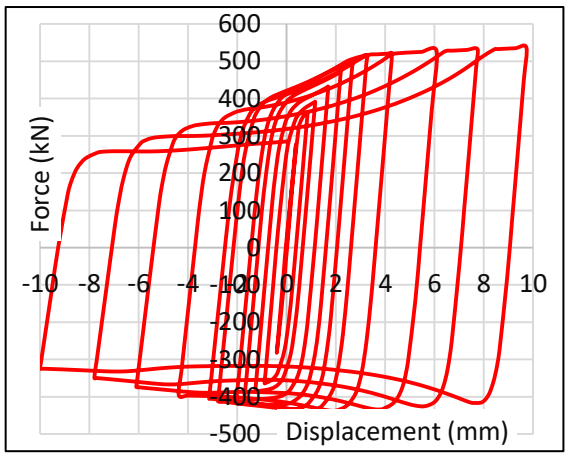

Fig. 8. Hysteresis Loops of CB with CDD.

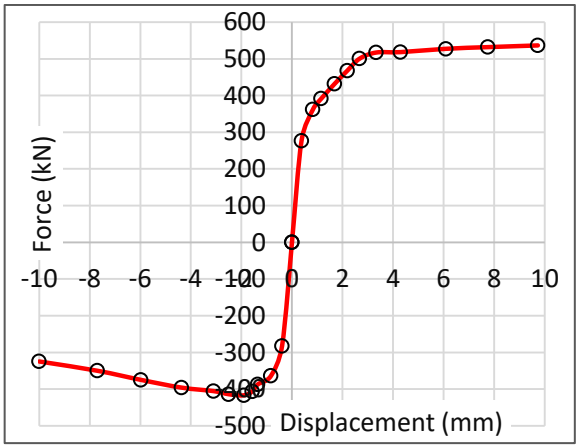

Fig. 9. Hysteretic envelope of CB- CDD.

Von misses stress contour Fig. 10 indicates that CDDs are functioning as the front-line fuse restricting damage to dissipative elements, while Fig. 11 represents displacement contour.

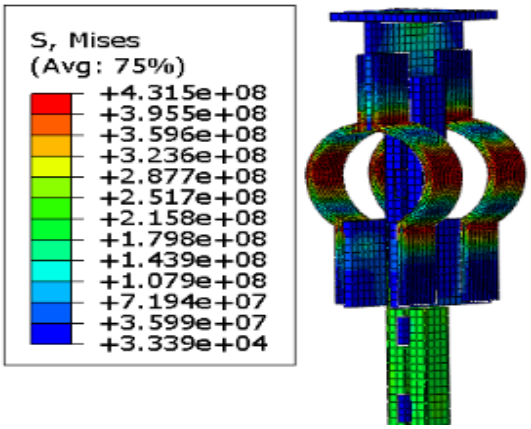

Fig. 10. Von Misses stress developed in CDD.

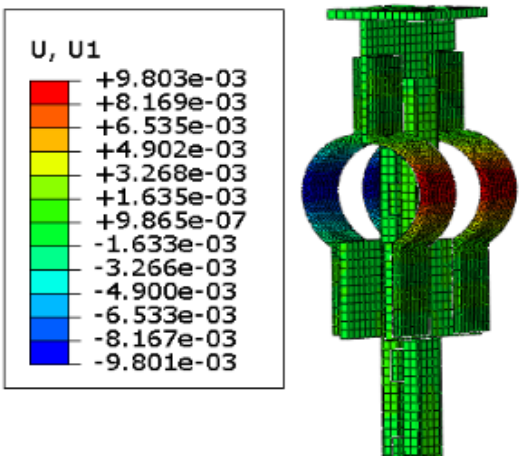

Fig. 11. Displacement contour of CDD.

The hysteresis envelop displays the tolerable tensile load achieved to 536.5 kN indicating the maximum capacity of the brace channels, while the tolerable compressive load in the nonlinear zone is 405.5 kN limited to the maximum capacities of the CDDs Fig. 9. In addition, maximum displacement reached at 97.31 mm in tension and 97.8 mm in compression.

Therefore, the mechanism has effectively created plastic hinges in CDDs and prevent the brace to buckle in compression Fig. 12. The brace channels in tension yield before the CDDs yield, that means the full functionality of the brace is utilized as proposed Fig. 13. One might raise the question of why the CDDs yielded in tension Fig 13, the answer is that only the surface elements of the plastic hinge rise the residual stress which displaced plastically under maximum compressional load.

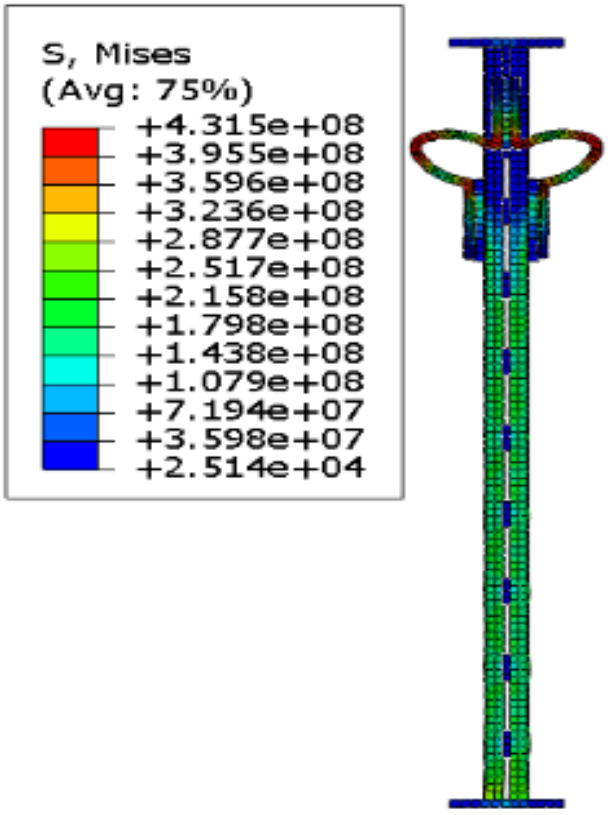

Fig. 12. Von Misses stress normal conditions

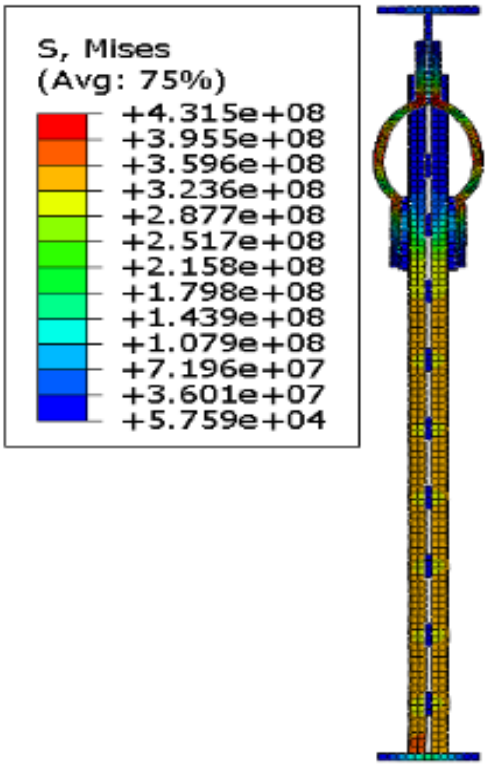

Fig. 13. max. stress in tension.

Fig. 14 demonstrates a considerable amount of energy dissipated by the structure. In addition, the hysteretic envelope Fig. 9 shows the maximum amount of displacement of 97.31 mm while the displacement at the end of the elastic zone is 2.7 mm. Thus, calculating the ductility factor (μ) is intended as;

$$\mu = \frac{\Delta max}{\Delta y} = \frac{97.3}{2.7} = 36.03 \quad (1)$$

So, another factor imperfects performance of the concentric brace satisfied as the ductility improved immensely.

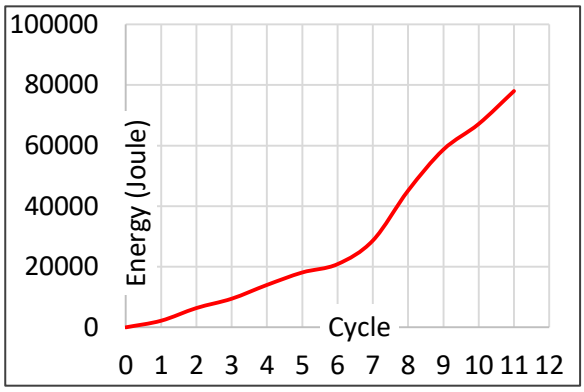

Fig. 14. Load-cycles- energy dissipated for model CB-CDD.

The ratio of nonlinear to linear bearing capacity of concentric brace with dissipator is 1.94. In addition, the ratio of dissipated energy in the last nonlinear to linear loading cycle is 35.7.

Table 2. Result comparison of models TCB and CB-CDD.

MODEL	E_{P-max} (JOULE)	E_{E-max} (JOULE)	P_{P-max} (KN)	P_{E-max} (KN)	$\frac{E_{P-max}}{E_{E-max}}$	$\frac{P_{P-max}}{P_{E-max}}$	$\frac{(\frac{E_P}{E_E})_{max}}{(\frac{P_P}{P_E})_{max}}$
CB-CCD	77980.6	2184.4	536.5	277	35.7	1.94	18.4
TCB-NO FUSE	51251.8	3756.3	542	483	13.64	1.12	12.18

EP-max : Energy value in the last nonlinear cycle

EE-max : Energy value in the last linear cycle

PP-max : Force value in the last nonlinear cycle

PE-max : Force value in the last linear cycle

$\frac{E_{P-max}}{E_{E-max}}$: The ratio of energy in the last nonlinear cycle to energy in the last linear cycle

$\frac{P_{P-max}}{P_{E-max}}$: The ratio of force in the last nonlinear cycle to force in the last linear cycle

By other means, the dissipated energy in the last nonlinear cycle is 35.7 times more than the energy dissipation in the last linear cycle. Displacement to cycle plot is presented in Fig. 15.

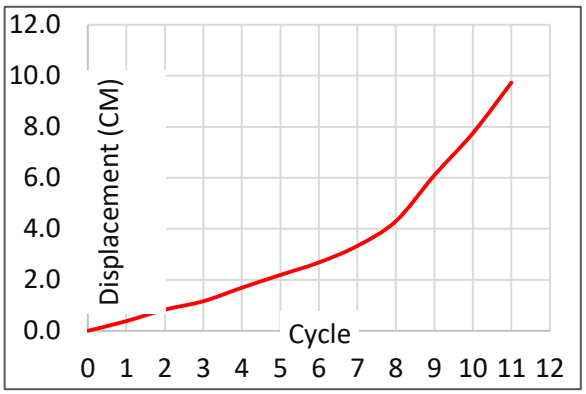

Fig. 15. Displacement. – loading cycles plot for model CB-CDD.

The overall nonlinear to linear dissipated energy ratio proportion to the nonlinear to linear bearing capacity is 35.7 as presented in Table 2.

In addition, force to energy ratio presented in Fig. 16 displays that the energy gradient curve increases at late loading cycles. The late steepness of the gradient curve represents the dissipation of an enormous amount of energy in proportion to the tiny variation of load. The plot of cumulative dissipated energy to the number of cycles also steeped at late cycles.

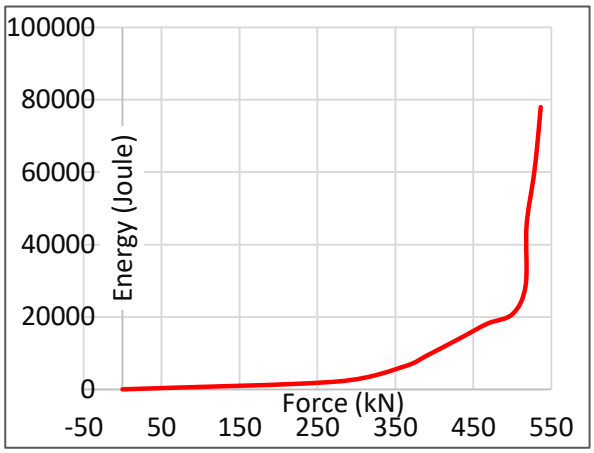

Fig. 16. Force-energy plot of CB-CDD.

Fig.17 demonstrates the amount of cumulative energy per loading cycle for model CB-CDD. The late steepens indicate the functionality of the plastic hinges.

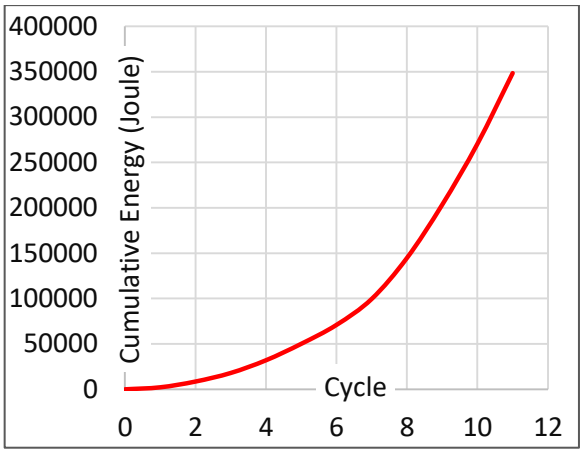

Fig. 17. Load cycles-cumulative energy.

The same analytical process was performed for TCB and compared the result with the CB-CDD model. The hysteresis loops for TCB are presented in Fig. 18.

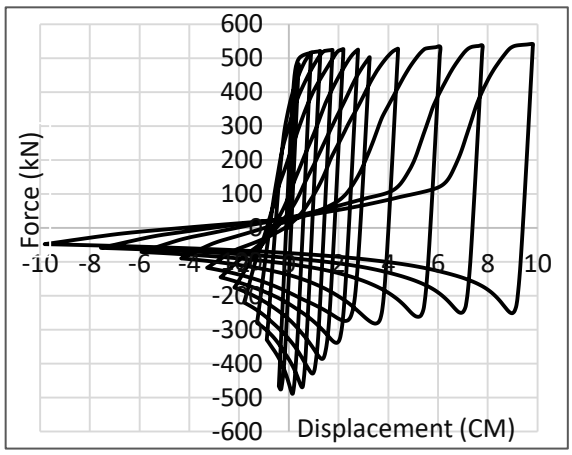

Fig. 18. Hysteresis loops for model TCB.

Fig. 18 and 19 exhibit the maximum bearable tensile capacity for TCB while critical force at compression caused the brace to buckle.

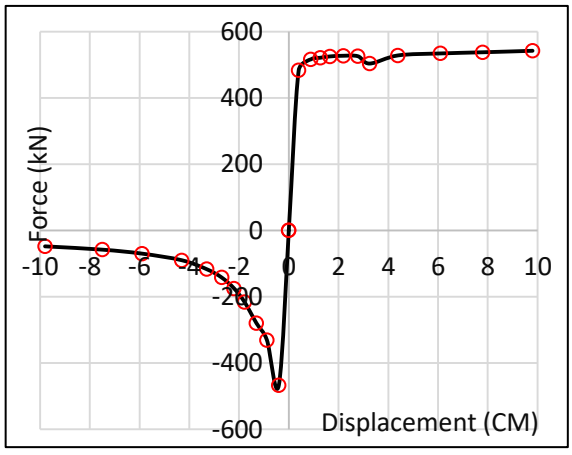

Fig. 19. Hysteretic envelope for model TCB.

Since, the anticipated plan was to retain the tensile original capacity of the concentric brace while improving its compressive performance, while the compressive bearing capacity of model TCB displays only 46.6 kN at the displacement of 9.66 cm. However, tensile performance demonstrates the same capacity and behaves under cyclic load as the CB-CDD model Fig. 19. Comparing the energy-load cycles for model TCB presented in Fig. 20 to Fig. 14 displays decline for TCB.

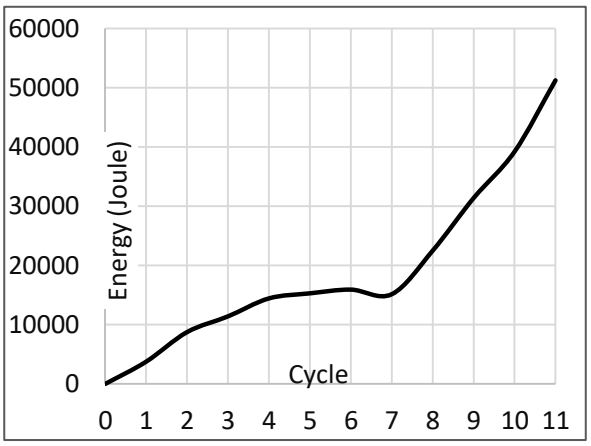

Fig. 20. Energy-cycles plot for model TCB.

The gradient of the curve increases when the load intensifies and drop of energy dissipation caused by the buckle.

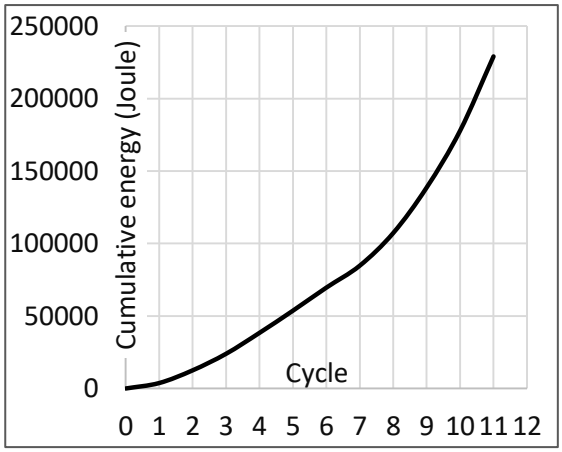

Fig. 21. Cumulative dissipated energy- load cycles for model TCB.

However, the energy dissipation dropped in the 6th and 7th cycles because the brace incompression yields nonlinearly Fig. 20. The loading cycles are associated with the cumulative energy presented in Fig. 21. Even

though the tolerable compressive capacity of the brace is considerably reduced in late cycles, the energy dissipation is still amplified because of the increased displacement.

Table 3. Result comparison of force-loading cycles and energy.

Model	Model CB with CDD	TCB
$\Delta_{P\,max}(CM)$	9.73	9.8
$\Delta_{E\,max}(CM)$	0.4	0.4
$\sum_{i=1}^{n} E_i\ (J)$	348516.1	229082.6
$\sum_{i=1}^{m} E_i\ (J)$	2184.4	3756.3
$\frac{\Delta_{P\,max}-\Delta_{E\,max}}{\Delta_{E\,max}}$	23.3	23.5
$\hat{E}_P = \frac{(\sum_{i=1}^{n} E_i - \sum_{i=1}^{m} E_i}{(n-m)}$	34633.17	22532.63
$\hat{E}_E = \frac{\sum_{i=1}^{m} E_i}{m}$ (J)	2184.4	3756.3
$\frac{\hat{E}_P}{\hat{E}_E}$	15.85	6.0

$\boldsymbol{\Delta_{P\,max}}$: Axial displacement of brace in the last nonlinear cycle

$\boldsymbol{\Delta_{E\,max}}$: Axial displacement of brace in the last linear cycle

$\sum_{i=1}^{n} E_i$: Total energy in 10 loading cycles

$\sum_{i=1}^{m} E_i$**:** Total energy in 1 loading cycle

$\hat{E}_P = \frac{(\sum_{i=1}^{n} E_i - \sum_{i=1}^{m} E_i}{(n-m)}$: Dissipated energy per loading cycle in nonlinear zone

$\hat{E}_E = \frac{\sum_{i=1}^{m} E_i}{m}$ (J): Dissipated energy per loading cycle in linear limit zone

$\frac{\hat{E}_P}{\hat{E}_E}$: The ratio of dissipated nonlinear energy to linear energy per loading cycles

7. Result and performance comparison of models CB-CDD and TCB

Hysteresis loops of concentric brace equipped with yielding elements are presented in Fig. 7. The maximum tolerable tensile capacity for both models is well matched. The method of displacement controlled cyclic load with maximum displacement amplitude of 100 mm was applied to evaluate the models' cyclic performance. The same technique is used to compare the cyclic performance of TCB and CB-CDD Fig. 24.

The capacity of energy consumption for models TCB and CB-CDD is compared in Fig. 22.

Therefore, the analytical result of model CB-CDD presents 1.73 times more tolerable capacity than TCB. As anticipated the same tensile capacity for TCB and CB-CDD models denotes the full utilization of the tensional functionality of the brace Fig. 24, while the compressive behavior of the CB-CDD model considerably improved. In terms of energy dissipation, the brace with dissipator absorbed 348516.1 J.

whereas the traditional concentric brace dissipated only 229082.6 J. Thus, the improved model dissipates 1.52 times more earthquake energy compares to the TCB model.

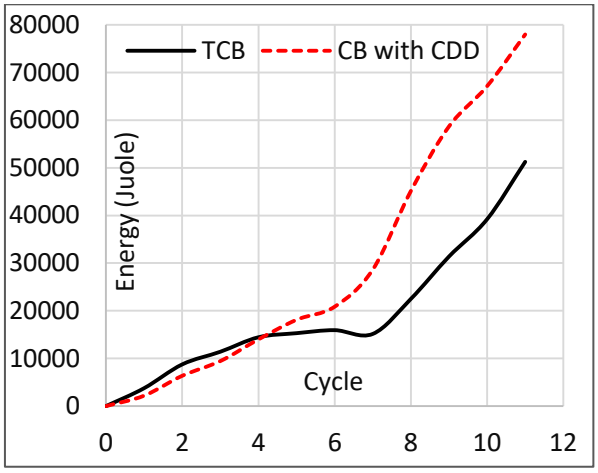

Fig. 22. Cycle-energy comparison for models TCB and CB-CDD.

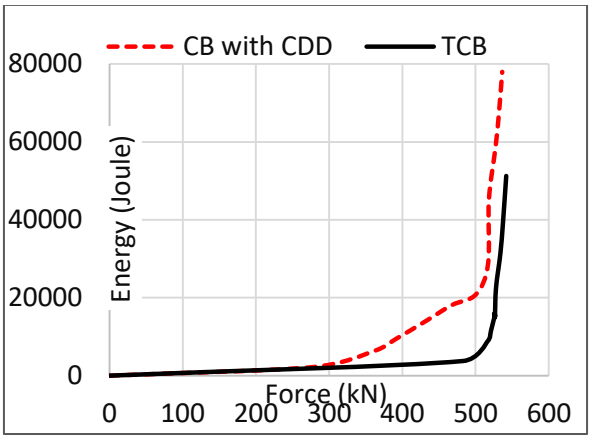

Fig. 23. Tensile force-energy compared for models TCB and CB-CDD.

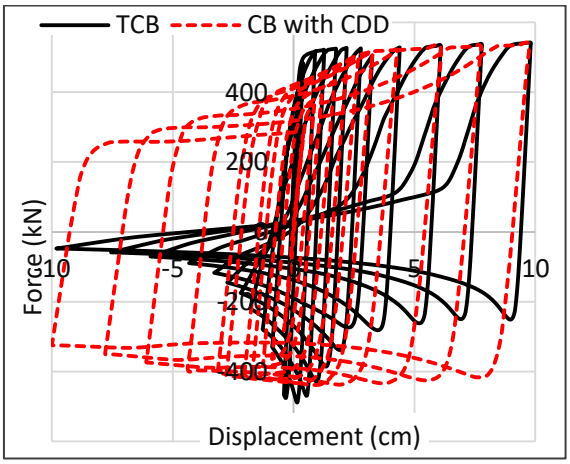

Fig. 24. Hysteresis loops comparison between TCB and CB-CDD.

The obtained force value of 536.5 kN for CB-CDD under cyclic loading dissipated 348516.1 J. energy, while the maximum force obtained by model TCB is 537 kN, and the energy dissipated 229082.6 J. Even though the tensional side for both models is designed to achieve the same performance in compression, however, the improved CB-CDD model dissipated 52.14% more energy.

The cycle to displacement plot shows that both models behave pretty much the same and no need to strengthen the CB-CDD model for improved performance.

8. Conclusions

The proposed goal of this research is to assess a concentric brace equipped with c-shaped dissipative devices to improve compressional behavior but maintain the tensional capacity of the brace. Therefore, the concentric brace with the yielding elements demonstrates enhanced ductility and improved cyclic performance while presented a similar tensile behavior.

Low cost of construction and ease of replacement and installation of the dissipative devices represent further advantages. A comparison of the obtained performance results for both models show effective role of the dissipative devices in CB-CDD acting as a first-line defensive fuse against earthquakes.

The value of energy dissipated by the CB-CDD is 1.52 times more than the TCB, also acting as the first line of defense against earthquake shakes helped the main structure to maintain its tolerable capacity. In other words, the studied CDD dissipated an enormous amount of earthquake energy, prevented buckling, and represented improved performance behavior. More predominantly, opposite to other performance improving methods, CDDs lets the brace to utilize its full tensional tolerability.

References

[1] Chittur Krishna Murthy AN. Application of visco-hyperelastic devices in structural response control 2005.

[2] Andalib Z, Ali Kafi M, Bazzaz M, Momenzadeh S. Numerical evaluation of ductility and energy absorption of steel rings constructed from plates. Eng Struct 2018;169. https://doi.org/10.1016/j.engstruct.2018.05.034.

[3] Chan RWK, Albermani F. Experimental study of steel slit damper for passive energy dissipation. Eng Struct 2008;30:1058–66. https://doi.org/10.1016/j.engstruct.2007.07.005.

[4] Marshall JD, Charney FA. A hybrid passive control device for steel structures, I: Development and analysis. J Constr Steel Res 2010;66:1278–86. https://doi.org/10.1016/j.jcsr.2010.04.005.

[5] Marshall JD, Charney FA. A hybrid passive control device for steel structures, II: Physical testing. J Constr Steel Res 2010;66:1287–94. https://doi.org/10.1016/j.jcsr.2010.04.002.

[6] Mansouri I, Safa M, Ibrahim Z, Kisi O, Tahir MM, Baharom S, et al. Strength prediction of rotary brace damper using MLR and MARS. Struct Eng Mech 2016;60:471–88. https://doi.org/10.12989/sem.2016.60.3.471.

[7] Hadianfard MA, Khakzad AR. Inelastic buckling and post-buckling behavior of gusset plate connections. Steel Compos Struct 2016;22:411–27. https://doi.org/10.12989/scs.2016.22.2.411.

[8] Bazzaz M, Kheyroddin A, Kafi MA, Andalib Z. Evaluating the performance of steel ring in special bracing frame. Proc. 6th Int. Conf. Seismol. Earthq. Eng., 2011.

[9] Abbasnia R, Vetr MG, Ahmadi R, Kafi MA. An analytical and experimental study on the ductility of steel rings. Sharif J Civ Eng 2009;25:41–8.

[10] Andalib Z, Kafi MA, Bazzaz M. Using hyper elastic material for increasing ductility of bracing. 1st Conf. Steel Struct. 2nd Conf.

Appl. High-Strength Steels Struct. Ind. Tehran, Iran, December, Persian, 2010.

[11] Bazzaz M, Kheyroddin A, Kafi MA, Andalib Z. Evaluation of the seismic performance of off-centre bracing system with ductile element in steel frames. Steel Compos Struct 2012;12. https://doi.org/10.12989/scs.2012.12.5.445.

[12] Abbasnia R, Vetr MGH, Ahmadi R, Kafi MA. Experimental and analytical investigation on the steel ring ductility. Sharif J Sci Technol 2008;52:41–8.

[13] Pachideh G, Kafi M, Gholhaki M. Evaluation of cyclic performance of a novel bracing system equipped with a circular energy dissipater. Structures 2020;28:467–81. https://doi.org/10.1016/j.istruc.2020.09.007.

[14] Bazzaz M, Andalib Z, Kheyroddin A, Kafi MA. Numerical comparison of the seismic performance of steel rings in off-centre bracing system and diagonal bracing system. Steel Compos Struct 2015;19. https://doi.org/10.12989/scs.2015.19.4.917.

[15] Pachideh G, Gholhaki M, Kafi M. Experimental and numerical evaluation of an innovative diamond-scheme bracing system equipped with a yielding damper. Steel Compos Struct 2020;36. https://doi.org/10.12989/scs.2020.36.2.197.

[16] Drei A, Castiglioni CA, Calado L, Vayas I. Seismic behaviour of steel braced frames with ductile INERD™ connections. Int. Conf. Stab. ductility steel Struct. Lisbon, 2006, p. 969–76.

[17] Naghavi M, Rahnavard R, Thomas RJ, Malekinejad M. Numerical evaluation of the hysteretic behavior of concentrically braced frames and buckling restrained brace frame systems. J Build Eng 2019;22:415–28. https://doi.org/10.1016/j.jobe.2018.12.023.

[18] Hashemi A, Yousef-Beik SMM, Mohammadi Darani F, Clifton GC, Zarnani P, Quenneville P. Seismic performance of a damage avoidance self-centring brace with collapse prevention mechanism. J Constr Steel Res 2019;155:273–85. https://doi.org/10.1016/j.jcsr.2018.12.019.

[19] Peng X-T, Lin C, Cao Y-M, Duan W-X. Seismic Behaviors of the Composite Central Brace with Steel Ring Damper. Proc. 2018 7th Int. Conf. Energy Environ. Prot. (ICEEP 2018), Paris, France: Atlantis Press; 2018. https://doi.org/10.2991/iceep-18.2018.190.

[20] Abdollahzadeh G, Hashemi SM, Tavakoli H, Rahami H. Determination of Hysteretic Behavior of Steel End-Plate Beam-to-Column Connection with Mechanical and Neural Network Modeling. Arab J Sci Eng 2014;39:7661–71. https://doi.org/10.1007/s13369-014-1348-4.

[21] Setyowulan D, Susanti L, Wijaya MN. Study on the behavior of a one way eccentric braced frame under lateral load. Asian J Civ Eng 2020;21:733–9. https://doi.org/10.1007/s42107-020-00234-2.

[22] Sabelli R, Mahin S, Chang C. Seismic demands on steel braced frame buildings with buckling-restrained braces. Eng Struct 2003;25:655–66. https://doi.org/10.1016/S0141-0296(02)00175-X.

[23] Naghipour M, Salim Bahrami SR. Improving the seismic performance of eccentrically braced frames by using a ductile element. Struct Constr Eng 2017;4:18–27. https://doi.org/https://doi.org/10.22065/jsce.2017.77539.1075.

[24] Xu X, Zhang Y, Luo Y. Self-centering eccentrically braced frames using shape memory alloy bolts and post-tensioned tendons. J Constr Steel Res 2016;125:190–204. https://doi.org/10.1016/j.jcsr.2016.06.017.

[25] Kazemi M, Kafi MA, Hajforoush M, Kheyroddin A. Cyclic behaviour of steel ring filled with compressive plastic or concrete, installed in the concentric bracing system. Asian J Civ Eng 2020;21:29–39. https://doi.org/10.1007/s42107-019-00181-7.

[26] Bruneau M, Bhagwagar T. Seismic retrofit of flexible steel frames using thin infill panels. Eng Struct 2002;24:443–53. https://doi.org/10.1016/S0141-0296(01)00111-0.

[27] Hosseini Hashemi B, Behnamfar F, Ranjbaran F. Effects of local eccentricity of

connecting braces on nonlinear behavior of steel concentric brace connections. J Seismol Earthq Eng 2008;10:91–9.

[28] Kheyroddin A, Gholhaki M, Pachideh G. Seismic evaluation of reinforced concrete moment frames retrofitted with steel braces using IDA and pushover methods in the near-fault field. J Rehabil Civ Eng 2019;7:159–73.

[29] Bazzaz M, Kafi MA, Kheyroddin A, Andalib Z, Esmaeili H. Evaluating the seismic performance of off-centre bracing system with circular element in optimum place. Int J Steel Struct 2014;14. https://doi.org/10.1007/s13296-014-2009-x.

[30] Andalib Z, Kafi MA, Kheyroddin A, Bazzaz M. Experimental investigation of the ductility and performance of steel rings constructed from plates. J Constr Steel Res 2014;103. https://doi.org/10.1016/j.jcsr.2014.07.016.

[31] Boadi-Danquah E, MacLachlan D, Fadden M. Cyclic Performance of a Lightweight Rapidly Constructible and Reconfigurable Modular Steel Floor Diaphragm. Key Eng Mater 2018;763:541–8. https://doi.org/10.4028/www.scientific.net/KEM.763.541.

[32] Deihim M, Kafi MA. A parametric study into the new design of a steel energy-absorbing connection. Eng Struct 2017;145:22–33.

[33] Khonsari S V, England GL, Parvinnia SMH. Innovative structural joint to increase safety during earthquakes. Proc. 13th World Conf. Earthq. Eng. (13WCEE), Pap., 2004, p. 1–6.

[34] (ATC) USATC. ATC 24: Guidelines for Cyclic Seismic Testing of Components of Steel Structures. California: Applied Technology Council; 1992.